Nanoplastic from mechanically degraded primary and secondary microplastics for environmental assessments

Hind El Hadri, Julien Gigault, Benoit Maxit, Bruno Grassl, Stephanie Reynaud

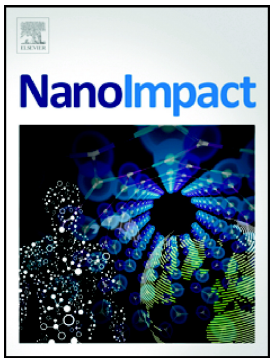

Nanoplastic from mechanically degraded primary and secondary microplastics for environmental assessments

Hind El Hadri, Julien Gigault, Benoit Maxit, Bruno Grassl, Stéphanie Reynaud

PII: S2452-0748(19)30115-6

DOI: https://doi.org/10.1016/j.impact.2019.100206

Reference: IMPACT 100206

To appear in: *NANOIMPACT*

Received date: 31 October 2019

Revised date: 20 December 2019

Accepted date: 20 December 2019

Please cite this article as: H. El Hadri, J. Gigault, B. Maxit, et al., Nanoplastic from mechanically degraded primary and secondary microplastics for environmental assessments, *NANOIMPACT*(2020), https://doi.org/10.1016/j.impact.2019.100206

Nanoplastic from mechanically degraded primary and secondary microplastics for environmental assessments

Hind El Hadri[1,3], Julien Gigault[2*], Benoit Maxit[3], Bruno Grassl[1*], Stéphanie Reynaud[1]

[1]CNRS/ Univ Pau & Pays Adour/ E2S UPPA, Institut des sciences analytiques et de physicochimie pour l'environnement et les matériaux, UMR 5254, 64000, Pau, France
[2]Géosciences Rennes, UMR 6118, CNRS – Université de Rennes 1, Av. Général Leclerc, Campus de Beaulieu, 35000 Rennes France
[3]Cordouan Technologies, Av. Canteranne, 33600, Pessac, France.

*Corresponding author: bruno.grassl@univ-pau.fr; julien.gigault@univ-rennes1.fr

Electronic supplementary information (ESI) available.

Abstract

Degradation of plastic waste in the environment leads to the formation of microplastics and nanoplastics. To better understand the fate, behavior and reactivity of nanoplastics, it is essential to conduct experiments with representative and well-characterized nanoplastics. In the present study, we provided a top down method based on mechanical degradation to obtain nanoplastics from both primary and secondary microplastics. These nanoplastics were then characterized in terms of size distribution, morphology and surface charge. It was found that they are highly polydisperse with different shapes and negatively charged surfaces and therefore very close to natural colloid characteristics. These nanoplastics may share similarities with environmental nanoplastics as referred to their chemical nature and morphology. Their physicochemical properties have been studied *vs.* salinity, pH and temperature. ~~In addition, their ability to act as nano-carriers was assessed through lead adsorption.~~

Keywords: Nanoplastic formation, environmental behavior, colloid characterization

1. Introduction

Plastic pollution has been clearly demonstrated for microplastics (MPs) debris and fragments in marine and freshwater systems [1–3]. However, degradation (by UV, biological organisms, mechanical phenomenon, etc.) of plastic debris is not expected to stop at the microplastic level. Interest in nanoplastics has therefore grown, with the main focus on bioaccumulation and eco-toxicological studies [4–8]. The formation of nanoplastics by degradation was demonstrated on polyethylene (PE) and polypropylene (PP) MP fragments under UV irradiation [9] and on disposable polystyrene (PS) cup lids using a weathering chamber [10] or via mechanical breakdown [11]. Moreover, to confirm this ascertainment, the presence of nanoplastics in the environment was recently detected in the north Atlantic gyre [12]. No definition of nanoplastics has been officially established, however, there is a growing tendency to report nanoplastics as unwanted products of plastic degradation with sizes ranging from 1 nm to 1 µm having a colloidal behavior (according to the Brownian definition) [7,13]. Nanoplastics may have a greater impact than MPs due to their dimensions and specific colloidal properties since they might cross biological barriers [14] and potentially become hazardous for living organisms [15]. Moreover, the nanoplastic high surface area would increase interactions with other contaminants (organic pollutants [16–24], trace elements [25,26]) and with natural colloids (inorganic colloids, organic matter, biopolymers) [27–31].

Studies dealing with both the impact and the behavior of nanoplastics were so far mostly performed using polystyrene latex particles (PSLs) due to its commercial availability in the nano size range. PSLs are synthesized (bottom-up approach) to be monodisperse and spherical. Such nanomaterials can mimic nanoplastics on the basis of size but the representativeness of their shape is debatable knowing that the particle morphology can play an important role in the heteroaggregation phenomena and the nanoplastic final environmental impact [27,30,32,33]. These PSLs are usually obtained via water-dispersed processes and formulated with additives such as surfactants and preservatives. More precisely, they are frequently stabilized by ionic or non-ionic surfactants such as Tween 20 and sodium dodecyl sulfate (SDS) and/or functionalized with carboxylate, amino or sulfate groups during the synthesis. Preservatives such as sodium azide are often used as antimicrobial agents. Pikuda *et al.* highlighted the importance of *(i)* performing control experiments to assess the effect of additives and *(ii)* washing the nanoplastic suspensions to remove any preservatives and avoid any bias when performing toxicity studies [34].

Recently, several studies focused on improving the representativeness of nanoplastic samples to investigate their fate and behavior in environmental media as well as their toxicity towards living organisms. Balakrishnan *et al.* developed a simple method to obtain PE nanoplastics using nanoprecipitation of a PE toluene solution. The improvement compared to previously described PSLs was the use of PE and bio-resource surfactants [35]. Rodriguez-Hernandez *et al.* also used nanoprecipitation to produce polyethylene terephthalate (PET) nanoplastics from fine chips of PET [36]. Mitrano *et al.* synthesized metal-doped nanoplastics to be used as tracers. They offer the advantage of being easily detected with accuracy and reliability in complex systems [37]. Pessoni *et al.* synthesized nanoplastics with different surface functionalities using a soap free emulsion polymerization (6–7 and 43–45 carboxylic groups per nm^2). These nanoplastics exhibited smooth or raspberry-like surface morphologies, and were monodisperse in size (PDI < 0.05) [38]. Following another strategy, Magri *et al.* described a top-down approach based on laser ablation to obtain PET nanoplastics. These nanoplastics had an average dimension of 100 nm after filtration, with significant size and shape heterogeneity (compared to polymerization in dispersed media), and weak acid groups at the particle surface [39]. Recently, Astner *et al* developed a top-down process by mechanical degradation to produce MPs and NPs from agricultural plastics (a mulch film prepared from biodegradable polymer polybutyrate adipate-co-terephthalate and low-density PE) [40].

Within this context, the current study describes an alternative top-down process to obtain fragmented nanoplastics approaching environmentally occurring nanoplastics. They were produced by mechanical degradation of commercially available primary MPs and secondary MPs (collected on beaches). The fragmented nanoplastics were then characterized using a complete nanoscale dedicated analytical strategy. This characterization was followed by a study of their physicochemical properties against parameters including ionic strength, pH and temperature. ~~At last, the behavior of this new class of Nanoplastics has been evaluated as pollutant carriers through the study of lead (Pb) adsorption on Nanoplastics.~~

2. Materials and methods

2.1 Materials

Deionized water (18 MΩ cm) was supplied by a Millipore water purification system (Merck, Darmstadt, Germany) and was used for all sample preparations and dilutions. Sodium hydroxide (NaOH) granules and hydrochloric acid (HCl) at 37 % from Sigma Aldrich (Lyon,

France) were used to prepare solutions at 0.1 and 0.01 mol L^{-1}. Sodium chloride (NaCl) ~~and salt of lead nitrate ($Pb(NO_3)_2$)~~ was purchased from Sigma Aldrich. Cellulose acetate filters (5-6 µm pore size) were purchased from VWR (Briare, France).

2.2 Sample preparation

Plastic materials

Nanoplastics were obtained by a top-down mechanical degradation of: *(i)* manufactured microplastics MPs (pellets for polystyrene, PS and powder for low molecular weight polyethylene, PE) purchased from Goodfellow (Lille, France) and Total (Paris, France) and *(ii)* unintentionally formed MPs (Table S1). The latter were plastic fragments (secondary MPs already degraded in the environment) collected on Guadeloupe beaches (16°21'06"N 61°23'09"W) in 2016 and named Gu-MPs (Figure S1). Guadeloupe is a French Caribbean island exposed to the north Atlantic gyre well known to be a zone of plastics accumulation [41].

Protocol for nanoplastic formation

For pellets and plastic fragments (size > 1 mm) a pre-degradation step was performed using a blade grinder to get a primary powder (the degradation steps are described in Figure S2). The final fragmentation for nanoplastic production was performed using a planetary ball mill (Pulverisette 7) from Fritsch GmbH (Idar-Oberstein, Germany). The tested zirconium oxide ball sizes were 0.5 mm, 1 mm, 5 mm and 10 mm in diameter. The optimized grinding duration and speed were found to be 120 min and 450 rpm respectively. The grinding process included 4 steps each composed of 10 cycles of 3 minutes of grinding and 6 minutes of pause. The first step was performed in dry conditions and the other steps in wet conditions using ethanol as a dispersant. At the end, a powder was obtained after drying the sample under vacuum to remove any trace of ethanol. The powder was then dispersed in water by bath sonication and filtrated to obtain submicronic particles (Figure S3). It should be noted that the filtration step can be critical since the plastic particles have a high affinity with polymeric membrane of commonly used filters. To reduce particle loss during the filtration, membranes with pore sizes greater than 1 µm (around 5-6 µm) were used.

The fragmented samples have been characterized by ATR-Infrared (Nicolet iS 50 FTIR, Thermo Fischer, Waltham, MD, USA) and scanning electronic microscopy (SEM, SH-3000 Hirox, Limonest, France). A total organic carbon instrument (Shimadzu, Kyoto, Japan) was used on the dispersion after filtration to determine the organic carbon concentration. In this article, the samples are named nano-PS and nano-PEs for the nanoplastic samples obtained

from the manufactured polystyrene and polyethylene (Table 1). nano-Gu is the denomination of the nanoplastics obtained from the secondary Gu-MPs.

~~*Sample preparation for the adsorption experiment*~~

~~For this experiment, to 4.7 ± 0.5 mg L^{-1} of PS-NPT batch, a solution of $Pb(NO_3)_2$ was added to reach a final Pb concentration of 6.6 ± 0.3 mg L^{-1} without significantly diluting the initial sample. The pH was not adjusted prior to sample analysis and was around 6.0 ± 0.5.~~

2.3 Instruments

Transmission electron microscopy (TEM) and Scanning electronic microscopy (SEM)

TEM images were obtained using an LVEM5 instrument (Delong Instrument, Brno, Czech Republic). It is a low voltage bench-sized transmission electron microscope with a Schottky field emission gun. It operates at a nominal acceleration voltage of 5 kV. Samples were prepared by directly placing 5 µL of suspension on 300 mesh ultrathin carbon film copper grids (Cu300-HD, Pacific Grid Tech, San Francisco, CA, USA) previously treated with glow discharge using an ELMO system (Cordouan Technologies, Pessac, France) to make the carbon membrane hydrophilic. After removing excess water using a flat filter paper, the TEM grids were air dried at room temperature for 10 minutes prior to analysis.

SEM images were obtained with a SH-3000 Hirox (Limonest, France) after metallization with gold using 30 mA for 60s (desk V, Denton Vacuum, Moorestown, NJ, USA). The accelerated voltage was 25 kV.

Dynamic light scattering (DLS)

Hydrodynamic diameters were determined using a contactless (*in situ*) DLS probe (Vasco flex) from Cordouan Technologies at 170°. The intensity fluctuations as a function of the time were processed as an autocorrelation function. Cumulants and Sparse Bayesian Learning (SBL) algorithms were used to fit this function in order to obtain a size distribution. Cumulants allow one to have the average diameter (z-average) while SBL provides a multimodal analysis with several hydrodynamic diameters.

Flow field flow fractionation (AF4)

An Eclipse 3+ AF4 system (Wyatt Technology, Santa Barbara, CA) was used as a separation system. It was equipped with a 1200 series UV-vis absorbance detector (Agilent Technologies, Les Ulis, France) and a multi-angle laser light scattering (MALS) detector (DAWN HELEOS, Wyatt Technology). The AF4 nominal (trapezoidal) channel height was established using a spacer of 250 µm (with dimensions of 26.5 cm length and narrowing

width from 2.1 to 0.6 cm). Polyethersulfone (PES) 10 kDa membranes were purchased from Wyatt Technology and used as the accumulation wall. Mobile phase flow was generated using a 1200 series pump (Agilent Technologies). All injections were performed with an Agilent Technologies 1260 ALS series autosampler. Data from the AF4 detectors were processed using Astra 6.1.7.17 (Wyatt Technology) and OpenLab (Agilent Technologies) software. The radius of gyration (R_g) was determined using the Berry formalism (first order) to analyze MALS data at different angles. The AF4 methods used here were based on a previous study [42] (Table S2). First, a global method with decreasing cross flow was used to rapidly determine the presence of submicron populations. Then to increase the resolution, specific methods with a constant flow rate were selected according to the size distribution obtained from the global method (Table 2).

~~To study the adsorption of Pb on Nanoplastics, AF4 was coupled to an ICP-MS 7500ce model (Agilent technologies, Tokyo, Japan). Before analysis, the ICP-MS was tuned using a multi-element standard solution (1 µg L^{-1} each of Li, Y, Tl and Ce in 2 %v/v HNO_3) to optimize the instrument for maximum sensitivity and minimum oxide ($^{156}CeO/^{140}Ce$) and doubly charged ($^{70}Ce^{++}/^{140}Ce^{+}$) levels (< 2 %). Data were collected at m/z 206, 207 and 208 for Pb in time resolved analysis mode with an integration time of 0.1 s.~~

Zeta-potential ζ

The surface charge of the particles was assessed using a Wallis zetameter from Cordouan Technologies (Pessac, France). The Wallis zetameter measures the electrophoretic mobility of colloidal particles by laser Doppler electrophoresis. Then a model (Smoluchowski) was used to calculate ζ. Prior to analysis, the pH and conductivity of samples were measured using a lab 850 pH-meter and lab 970 conductivity-meter from SI Analytics (Xylem, Weilheim, Germany) respectively. To avoid any misinterpretation, distinct native solutions were employed when acidifying with HCl and basifying with NaOH to limit the increase in ionic strength due to additive Na^+ and Cl^- concentrations during zeta-potential measurements.

3. Results and discussion

3.1 Fragmented nanoplastic by top-down process

Primary and secondary materials were grinded within two steps using successively a blade grinder and a planetary ball mill (mechanochemistry of polymer [43]). For the latter, zirconium oxide was chosen as constitutive material for the bowls and balls by taking into

account its density and abrasion resistance. Additionally, the effect of the ball size was studied and sizes of 0.5 mm and 1 mm in diameter (compared to 5 mm and 10 mm) involved both the aggregation/agglomeration of the plastic material and a decrease in nanoplastic concentration (Figure S4). Both the grinding duration and speed were optimized to prevent any temperature increase and avoid reaching the melting point of the plastic material. The grinding process was thus divided in cycles including grinding and time-off periods. The temperature was measured in the plastic mixture after 3 min of grinding and was found to be below 62 ± 2 °C which is significantly below the melting points of all the polymers used in this study. The fragmentation was performed using ethanol as dispersing medium to get the lowest size distribution. The purification steps only included the removal of ethanol at the end of the process. SEM analysis of the in-process sample showed irregularities forming at the surface of the particles and the presence of outgrowths that might end up as nanoplastics (Figure S5).

The final fragmented sample of Guadeloupe MPs obtained from secondary materials (see experimental section) was mainly composed of PE and PP according to ATR-Infrared analysis (Figure S6). The carbonyl index, determined as the ratio between the carbonyl absorption band (1780-1600 cm^{-1}) and the methylene absorption band (1490-1420 cm^{-1}) [44], was 0.3 ± 0.1 meaning that the environmental sample was already aged (oxidized). Nanoplastics concentrations ranged from 40 to 70 mg L^{-1} as reported in Table 1.

To assess the reproducibility of the degradation process, several batches of nano-PSs were produced using the same protocol (grinding, sonication and filtration). The batches were characterized by DLS and AF4 to get the nanoplastic sizes and size distributions (Table S3, Figure S7). The z-average values were in the same size range with variability (relative standard deviation) below 10 %. The sample polydispersity was large as illustrated by the PDI (*i.e.* 0.16 ± 0.07 compared to 0.05 for a monodisperse sample [45]). The AF4 data from the different batches confirmed the reproducibility of the protocol as demonstrated by variabilities of the Rg (min, max and mean Rg) in the range of 10 to 16 %. The zeta-potential measured for several nano-PS and nano-PEs batches was systematically below -30 mV (in average -40 ± 5 mV and -37 ± 4 mV for PS and PE, respectively).

1: Description of the nanoplastic models used in this study

Sample name	Composition	Concentration (mg L^{-1})	z-average[a] (nm) ζ (mV)[d]	Global AF4 method		Specific AF4 methods	
				Mean[b] Rg (nm)	Rg maximum peak[c] (nm)	Mean[b] Rg (nm)	Rg maximum peak[c] (nm)
nano-PSs	Polystyrene	62 ± 6	306 ± 15 -44 ± 2	205	240	260	270
nano-PEs	Polyethylene	46 ± 5	129 ± 7 -38± 3	110	40	150	Peak 1: 40 Peak 2: 150
nano-Gus	Polyethylene/ Polypropylene	40 ± 5	460 ± 23 -30 ± 2	255	260	280	300

[a] determined with the Cumulant algorithm

[b] over the entire peak range

[c] at the maximum of the MALS peak

[d] in water at 25 °C, pH = 6.7±0.3, samples diluted 10 times

3.2 Nanoplastic morphology

The nanoplastic batches used for this study are listed in Table 1. First, the shape of the nanoplastics was assessed by TEM analyses. For all the samples, the particles were polydisperse, polymorphic and therefore very different from spherical monodisperse PSLs (Figure 1 and Figure S8). nano-PE sizes were much smaller (< 100 nm) than those of nano-PSs and nano-Gus. For nano-PSs and nano-Gus, two populations were observed on the TEM images: *(i)* one with well contrasted black cracked particles (white frames in Figure 1A and C) and *(ii)* a second with more anisotropic dark-grey particles (black frames in Figure 1A and C). This lower contrast of the second population could be explained by a lower particle thickness which, in turn, can be attributed to the peeling (instead of a breaking) of the MP surface. The heterogeneous shapes obtained for PS, PE and PE-PP (nano-Gus) particles were in accordance with those recently reported by Gigault *et al.* [9,13] obtained by UV degradation.

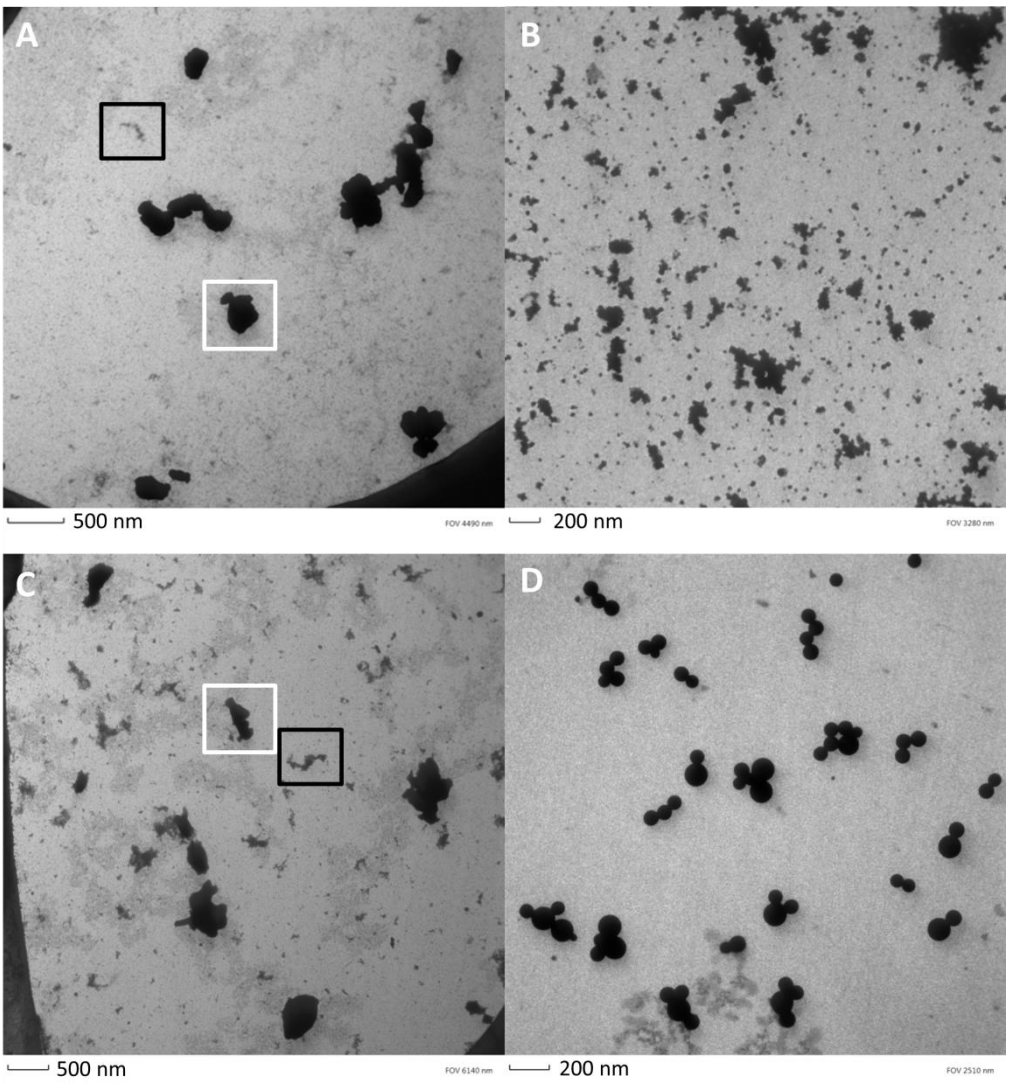

Figure 1 : TEM images of A) nano-PSs, B) nano-PEs and C) nano-Gus compared to D) a mixture of monodisperse PSL with sizes of 50 nm and 100 nm. The black and white frames (in A and C) show the difference in particle density.

3.3 Nanoplastic Size distribution

Size distributions of our nanoplastics (nano-PSs, nano-PEs and nano-Gus) were complementarily determined by DLS and AF4 as illustrated in Figure 2. DLS is a rapid and simple technique based on the Brownian motion of particles. It allowed us to get an overview of the average size and polydispersity of the sample, thus determining the submicronic characteristics of the sample. AF4 method was used to obtain a more resolved size distribution of the samples. Figure 2a and Table 1 show the hydrodynamic diameter distributions and the mean diameters (z-average), respectively. All nanoplastic samples were polydisperse and the nano-PE sample had the smallest plastic particles with a z-average of

129 nm. By converting the intensity-based to a number-based distribution the nanoplastic main population was below 100 nm (≈70 nm) as observed by TEM (Figure S9). The particle size distribution (Figure 2a) showed that the first population of nano-Gus was close to the nano-PS diameters whereas the second population of nano-Gus was around 800 nm explaining the shift of the z-average toward bigger sizes. Indeed, the z-average for nano-PSs was around 300 nm while for nano-Gus it was 460 nm (Table 1).

AF4 was then used to provide a complementary characterization of the size distributions of these polydisperse samples. The analytical method was based on a previous study [42]. In a first approach, a global method determined the presence of submicron populations. Then, specific methods were applied to enhance the resolution of the size separation in the size range determined by the global method. The detailed parameters of the different methods are reported in Table S2. The global method showed that the size distributions for nano-PSs and nano-Gus were comparable with a gyration radius (R_g) ranging from about 70 nm to 270 nm and 70 nm to 330 nm for nano-PSs and nano-Gus, respectively (Figure 2b). As reported in section 3.2, nano-PEs were smaller. Indeed, the main population (from 6 min to 12 min) had a Rg ranging from about 20 nm to 65 nm while the second minor population increased up to 330 nm. The AF4 global analysis was then followed by AF4 specific methods with constant flow rates: method B for nano-PSs and nano-Gus and method A for nano-PEs (Figure 2c). Size distributions (Rg) for nano-PSs and nano-Gus ranged from 120 nm to 330 nm and from 130 nm to 330 nm, respectively. For nano-PEs, the size distribution was larger with a Rg ranging from 20 nm to 380 nm. The average Rg over the entire signal was 260 nm, 280 nm, and 150 nm for nano-PSs, nano-Gus and nano-PEs, respectively (Table 1). At the maximum of the peak, Rg was 270 nm and 300 nm for nano-PSs and nano-Gus, respectively. For nano-PEs, two peaks were observed (Figure 2c) with a maximum signal around 10 min corresponding to Rg = 40 nm and at 26 min with Rg = 150 nm. The first peak showed that a high concentration of small particles (< 100 nm) was present in the sample. This could be explained by the low molecular weight of the initial PE-MPs (compared to other MPs Table S1) used for the degradation. The polymer chain may break more easily and then produce smaller particles. The second peak was due to higher sensitivity of MALS for large particles even though we still observed a size continuum. These results were in accordance with the DLS trend reported above.

Overall, nanoplastics obtained from mechanical degradation with different chemical composition were polydisperse with irregular particle shapes.

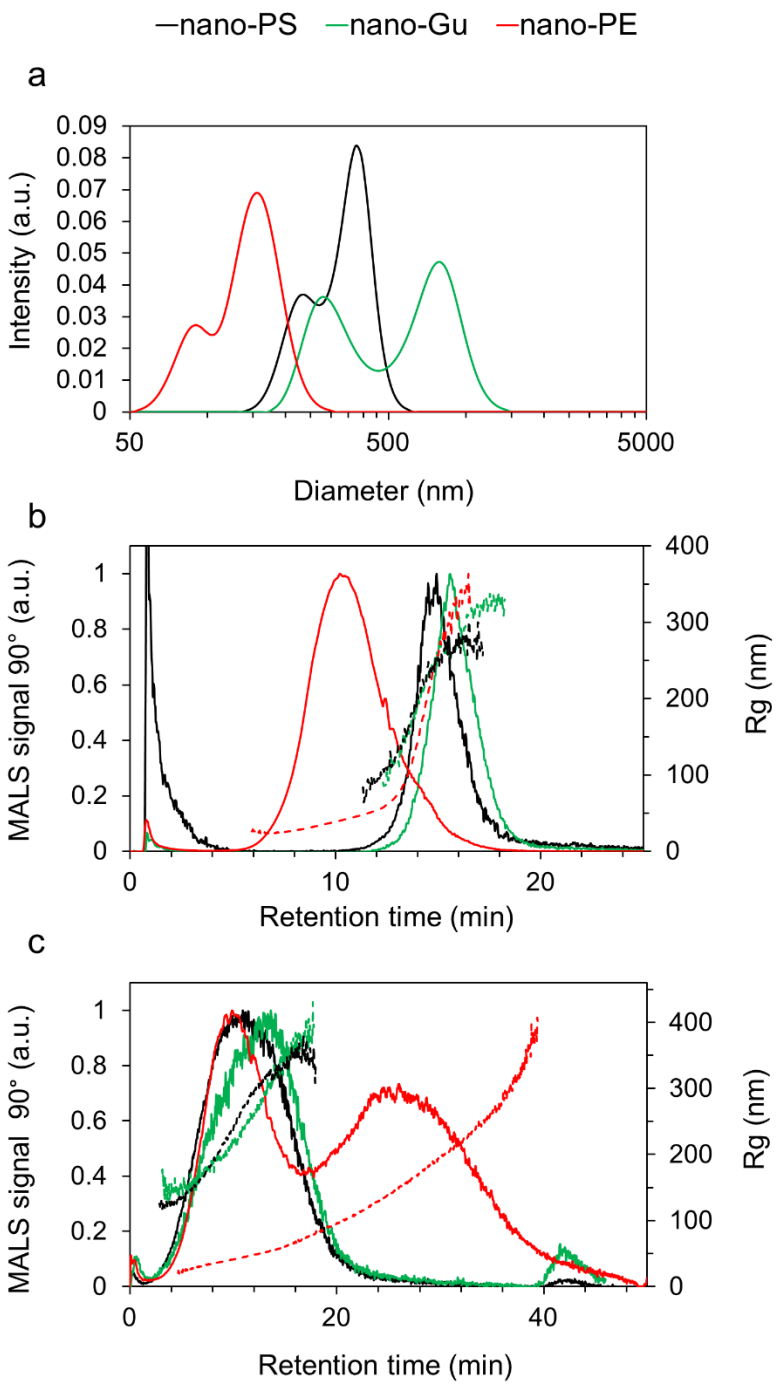

Figure 2: Size distribution of nano-PSs, nano-PEs and nano-Gus obtained by a) DLS with the SBL algorithm (hydrodynamic diameter) and obtained by AF4 coupled with multi-angle laser light scattering (MALS) signal with b) the global method and c) the specific methods (specific method A for nano-PEs and specific method B for nano-PSs and nano-Gus; Table S2). The radius of gyration (Rg) is represented by the dotted lines.

3.4 Surface characterization

Particle surface is an important parameter which can govern the nanoplastic interactions with contaminants and natural colloids in the environment as well as their physicochemical behavior. Nanoplastic surface charge was assessed by measuring the zeta-potential (ζ). ζ is also an appropriate indicator of the particle stability when it relies on the electrostatic repulsion: a high absolute zeta-potential (|ζ|) value usually indicates a better particle stability [46]. For all the samples, nanoplastics were negatively charged with |ζ| values of 44.0 ± 2.0 mV, 30.2 ± 1.1 mV and 38.0 ± 2.4 mV at native pH 6.4, 7.0, and 6.6 for nano-PSs, nano-Gus and nano-PEs, respectively. Therefore, the nanoplasic samples may be considered as electrostatically stable.

For nano-PSs, Figure 3a shows the influence of the dilution factor on |ζ| value from the initial concentration of 62 ± 6 mg L^{-1} (Table 1). No significant difference was observed with stable |ζ| around 45 mV regardless of the concentration. These results are in accordance with the literature which reported that the influence of particle concentration was negligible [47]. The same experiment was performed on nano-Gus where |ζ| increased significantly from 23.5 ± 1.7 mV to 33.7 ± 1.9 mV with increasing dilution factor (Figure S10). It is worth reminding that, nano-Gu sample came from the degradation of MPs collected on the field and these MPs were suspected to have aged in the ocean before being collected. Therefore, residues of salts were probably present as confirmed by the initial conductivity of the sample. For comparison, solution conductivity for crude samples was 257 ± 3 µS cm^{-1} and 57 ± 3 µS cm^{-1} for nano-Gus and nano-PSs respectively. By diluting the nano-Gu sample the ionic strength decreased and therefore |ζ| could be affected.

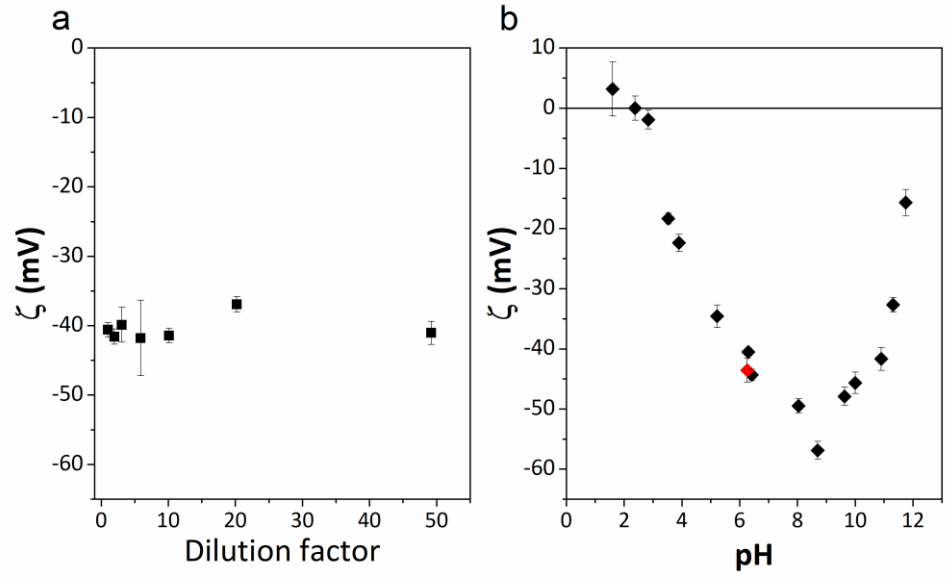

Figure 3: Zeta-potential of a nano-PS sample as a function of a) the dilution factor (C_0 = 62 ± 6 mg L^{-1}) and b) the pH

The native pH of the crude nano-PS sample (at 6 mg L^{-1}) was 6.4 ± 0.1. The influence of pH on the zeta-potential is presented in Figure 3b and three behaviors were observed:

(i) Reduction of pH involved a decrease of |ζ| from 44.0 ± 2.0 mV at pH 6.4 to 0 ± 2 mV at pH 2.4. It is worth mentioning that the positive value of 3.2 mV obtained at pH 1.6 is most likely due to the nanoplastic instability in this range of zeta-potential as confirmed by the high uncertainty on this measurement (± 4.5 mV).

(ii) Increase of pH from 6.4 up to 8.7 implied a |ζ| increase from 44.0 ± 2.0 mV to 56.9 ± 1.5 mV. Under this range of pH, the stability came from the deprotonation of the nanoplastic surface by NaOH yielding to more electrostatic repulsions.

(iii) Increase of pH above 9 implied a |ζ| decrease down to 15.7 ± 2.2 mV at pH 11.8. This behavior could be associated with a stability reduction despite the assumption that nanoplastics continued to be deprotonated.

It is well known that the increase of ionic strength (and therefore conductivity) affects the value of the zeta-potential (by modification of the double layer). To assess the effect of salt on the ζ value, NaCl was added to the nano-PS sample in order to obtain similar ionic strength than the one estimated for acidic and alkaline samples (Figure S11). It was observed that |ζ| curves with addition of NaOH or NaCl follow the same trend. Therefore, the |ζ| decrease observed in alkaline solutions can be attributed to the increase of ionic concentrations in the solutions rather than to the change in pH. The decrease of |ζ| was faster in acidic solutions than in both alkaline (NaOH) and salted (NaCl) solutions. Therefore, it confirmed that addition of H^+ species to the nano-PS samples decreased rapidly the stability by protonating the surface and making it more neutral (loss of electrostatic repulsion). |ζ| diminution with decreasing pH was consistent with the presence of weak acid groups on nanoplastics surface [39] which was confirmed by acid-base titration. The reduction of |ζ| was lower in alkaline and salted samples indicating that the species were more stable and should not aggregate as fast as in an acidic medium. The stability of our nanoplastics in these media was assessed in the section 3.5.

3.5 Nanoplastic stability

The understanding of the nanoplastic stability in different media is required to anticipate their suitability for environmental applications and to consider them as representative environmental nanoplastics (for instance studies on eco-toxicity, transport or heteroaggregation)[48]. The effects of ionic strength and pH on the stability of the nano-PSs were reported in section 3.4 using the zeta-potential values, the aggregation phenomenon is now evaluated using DLS measurements. In this section, three pH over a large range of values were selected: 2.8, 3.9 and 11.8 (in addition to the native pH 6.4). Additionally, two different salt concentrations were tested: 6 mmol L^{-1} and 13 mmol L^{-1} corresponding to ionic strengths close to groundwaters and freshwaters [49].

Figure 4 presents the autocorrelation functions (ACFs) of nano-PS samples spiked with HCl and NaOH to set the pH or with NaCl to fix the ionic strength. Analyses of these samples were performed at t_0 = 0 day, 5 days and 14 days (Figure 4) after spiking:

(i) After 5 days, ACFs of samples at pH above 3.9 and samples with fixed ionic strengths up to 13 mmol L^{-1} NaCl, were strictly similar to the initial nano-PS sample one, while at pH 2.8, ACF displayed a slower decay rate. The ACF trend at pH 2.8 is characteristic of a slower Brownian motion indicating that nano-PSs were unstable and aggregated. The particle aggregation kinetic was rapid at this pH *i.e.* within the first hour after addition of acid (Figure S12).

(ii) After 14 days, only ACF at alkaline pH (11.8) overlapped with the t_0 one meaning that the deprotonation of the particles increased their stability even if the zeta-potential value is only -15.7 ± 2.2 mV as previously explained. ACFs for acidic and salted samples presented a slower decay rate compared to t_0 ACF, meaning that aggregation occurred. Thus, the aggregation phenomenon decreased with the following order: pH 2.8 > NaCl 13 mmol L^{-1} > pH 3.9 > NaCl 6 mmol L^{-1} corresponding to the increase of $|\zeta|$ from 1.9 mV to 26.5 mV. As the zeta-potential value of stable particles obtained at pH 11.8 is included within this range, these results demonstrated that the zeta-potential value alone is not sufficient to assess the nanoplastic stability especially when different pH and ionic strength are studied.

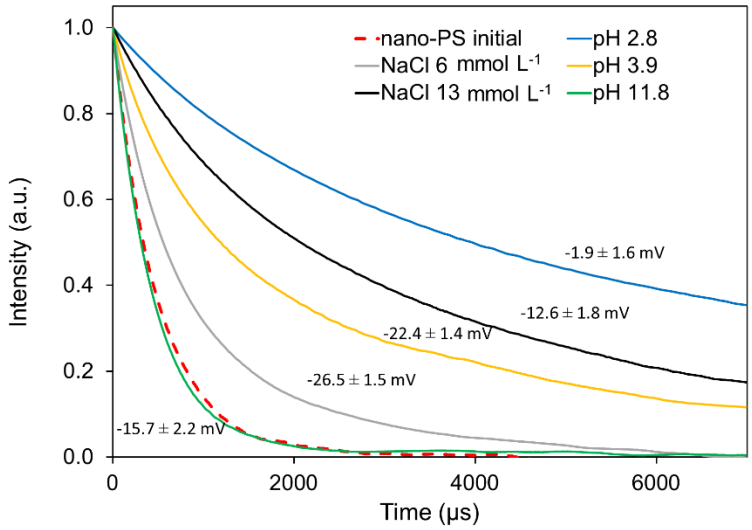

Figure 4: Autocorrelation function (g_2) of nano-PSs at different pH and concentrations of NaCl measured at 14 days. The zeta-potential values for each sample are reported on the graph.

In addition to pH and ionic strength, the storage conditions may have an effect on the stability of nanoplastic samples. The stability (assessed by the mean diameter) of the nano-PS as a function of time (14, 23 and 50 days), dilution factor (D1 = undiluted, D10 and D100 for 10 and 100 fold dilution) and storage temperature (T≈22°C and T≈4°C) was evaluated (Figure S13). At native nano-PS concentration (62 mg L^{-1}) z-average did not change regardless of the temperature and the storage duration. However, at lower concentrations (D10 = 6.2 and D100 = 0.62 mg L^{-1}), an increase of the diameter was observed for both temperatures. After 50 days, for D10, z-average increased by 51 % and 4 % at 22°C and 4 °C, respectively; and for D100, it was 210 % and 18 % higher than t_0 at 22°C and 4 °C, respectively. Therefore, it is preferable to keep the nanoplastic samples at their highest and native concentrations around 4 °C. It should be noted that bath sonication of the sample was able to re-disperse to some extent the nanoplastics (decrease in sizes by DLS). For instance, after 5 months storage at room temperature, the aggregation of nano-PEs was observed (increase of the diameter) and 15 min of bath sonication reduced the z-average of the sample from 510 nm to 170 nm.

In the current study, nano-PSs were found to be stable for at least a week before starting to aggregate in environmental pH range (values ranging from 4 to 9) as well as in freshwater-like ionic strengths (up to 13 mmol L^{-1}). Aggregation of nanoplastics in seawater could also be relevant in order to assess their toxicity to marine species and their transport in oceans. As expected and found in the literature [48,50,51], we observed fast aggregation (within 1 hour)

of nano-PSs in high salinity solutions (25 g L^{-1} of NaCl) (Figure S14a). The critical coagulation concentration of NaCl for a nano-PS sample was about 15 g L^{-1} (determined using DLS) (Figure S14b). The sample media can become more complex by adding natural colloids such as organic matter and clays. Usually, organic matter tends to stabilize nanoplastics in aquatic media [30,48].

~~**3.6 Example of application: metal adsorption**~~

~~Due to the NANOPLASTIC colloidal behavior and surface functionality, toxicity of these particles can be attributed to their ability to sorb, concentrate and transport pollutants such as trace elements. Lead (Pb) was selected based on our previous studies and because of its environmental toxicity. Samples were analyzed by AF4 coupled to UV-vis, MALS and ICP-MS detectors using the AF4 global method. In Figure 5, it can be observed that MALS and UV signals are similar in shape for both samples *i.e.* with and without Pb spiking. No change in size distribution appeared after adding Pb to the PS-NPT sample. Regarding the ICP-MS signal, no m/z 206 was detected in the blank solution of PS-NPTs alone whereas a peak at 15 min was observed in the sample spiked with Pb. Quantitatively, only 0.04 % (2.7 ± 0.4 µg L^{-1}) of the added Pb was adsorbed on the particles. It would represent a number of adsorbed Pb of 0.4 # nm^{-2} assuming that PS-NPTs had an equivalent spherical average diameter of 306 nm. In agreement with other works described in the literature, this experiment showed that Nanoplastics can adsorb lead on their surface and therefore are able to transport metals in the environment. The amount of adsorbed Pb was much lower in the current study (0.04 %) compared to Davranche *et al.* (about 90 %) probably due to the presence of organic matter which is known to increase the adsorption of heavy metals including Pb.~~

~~**Figure 5:** AF4-MALS-UV-ICP-MS fractograms of a PS-NPT sample without (black line) and with (red line) addition of Pb. The global AF4 method (Table 1) was used. a) MALS signal at 90° is reported (the radius of gyration (Rg) is represented by the dotted lines), b) UV signal at 254 nm and c) ICP-MS signal of isotope ^{206}Pb.~~

4. Conclusion

In this paper we proposed new manufactured nanoplastics from their top-down process to their characterization showing their relevance as environmental nanoplastic samples. Nanoplastics were prepared from mechanical degradation of various microplastics (PS, PE

and environmentally pre-degraded PE/PP) and were characterized in terms of size and size distribution (using DLS, AF4 and TEM), shape (TEM), surface charge (zeta-potential measurements) and environmental stability. The resulting nanoplastics were polydisperse (with sizes ranging from 20 nm and 1 µm), polymorphic (non-spherical plastic species) and negatively charged at pH ranging from 4 to 11. The fragmentation efficiency depends on the properties of the plastic (*e.g.* glass temperature, molecular mass) but also on the pre-degradation state of the plastic before the grinding process. Thus, HDPE and PP are difficult to degrade if they are pristine but after degradation in the environment they become more breakable by friction and impact as demonstrated in this study for PP and PE collected on Guadeloupe beaches.

The use of well-characterized nanoplastics is important for various environmental applications such as: the nanoplastic eco-toxicological effects, the environmental behavior and fate of various contaminants (adsorption of inorganic or organic pollutants on nanoplastics modifying their transport) or the assessment of heteroaggregation with natural colloids. This study reports an alternative way to obtain nanoplastic samples from controlled fragmentation of primary and secondary microplastics. Considering their size, morphology, chemical composition, these nanoplastics may be considered as relevant and representative "environmental" nanoplastics and are candidates of choice to study the impact and behavior of such species for future works within the domain.

Acknowledgements

We acknowledge funding and support from the Nouvelle-Aquitaine Region (En-Pi project). We would like also to thank Mr. Boris Pedrono from Cordouan Technologies (Pessac-France) for fruitful discussion.

References

[1] M. Bergmann, L. Gutow, M. Klages, Marine Anthropogenic Litter, Springer, 2015.
[2] C.B. Crawford, B. Quinn, Microplastic Pollutants, Elsevier, 2016.
[3] M. Wagner, S. Lambert, Freshwater Microplastics: Emerging Environmental Contaminants?, Springer, 2017.
[4] Nanoplastic should be better understood, Nature Nanotechnology. 14 (2019) 299. https://doi.org/10.1038/s41565-019-0437-7.
[5] S. Wagner, T. Reemtsma, Things we know and don't know about nanoplastic in the environment, Nature Nanotechnology. 14 (2019) 300–301. https://doi.org/10.1038/s41565-019-0424-z.
[6] M. Sander, H.-P.E. Kohler, K. McNeill, Assessing the environmental transformation

of nanoplastic through 13 C-labelled polymers, Nature Nanotechnology. 14 (2019) 301–303. https://doi.org/10.1038/s41565-019-0420-3.
[7] A.A. Koelmans, Proxies for nanoplastic, Nature Nanotechnology. 14 (2019) 307–308. https://doi.org/10.1038/s41565-019-0416-z.
[8] A.L. Dawson, S. Kawaguchi, C.K. King, K.A. Townsend, R. King, W.M. Huston, S.M. Bengtson Nash, Turning microplastics into nanoplastics through digestive fragmentation by Antarctic krill, Nature Communications. 9 (2018). https://doi.org/10.1038/s41467-018-03465-9.
[9] J. Gigault, B. Pedrono, B. Maxit, A.T. Halle, Marine plastic litter: the unanalyzed nano-fraction, Environ. Sci.: Nano. 3 (2016) 346–350. https://doi.org/10.1039/C6EN00008H.
[10] S. Lambert, M. Wagner, Characterisation of nanoplastics during the degradation of polystyrene, Chemosphere. 145 (2016) 265–268. https://doi.org/10.1016/j.chemosphere.2015.11.078.
[11] M.T. Ekvall, M. Lundqvist, E. Kelpsiene, E. Šileikis, S.B. Gunnarsson, T. Cedervall, Nanoplastics formed during the mechanical breakdown of daily-use polystyrene products, Nanoscale Advances. (2019). https://doi.org/10.1039/C8NA00210J.
[12] A. Ter Halle, L. Jeanneau, M. Martignac, E. Jardé, B. Pedrono, L. Brach, J. Gigault, Nanoplastic in the North Atlantic Subtropical Gyre, Environmental Science & Technology. 51 (2017) 13689–13697. https://doi.org/10.1021/acs.est.7b03667.
[13] J. Gigault, A. ter Halle, M. Baudrimont, P.-Y. Pascal, F. Gauffre, T.-L. Phi, H. El Hadri, B. Grassl, S. Reynaud, Current opinion: What is a nanoplastic?, Environmental Pollution. 235 (2018) 1030–1034. https://doi.org/10.1016/j.envpol.2018.01.024.
[14] K. Mattsson, E.V. Johnson, A. Malmendal, S. Linse, L.-A. Hansson, T. Cedervall, Brain damage and behavioural disorders in fish induced by plastic nanoparticles delivered through the food chain, Scientific Reports. 7 (2017). https://doi.org/10.1038/s41598-017-10813-0.
[15] R. Lehner, C. Weder, A. Petri-Fink, B. Rothen-Rutishauser, Emergence of Nanoplastic in the Environment and Possible Impact on Human Health, Environmental Science & Technology. 53 (2019) 1748–1765. https://doi.org/10.1021/acs.est.8b05512.
[16] I. Velzeboer, C.J.A.F. Kwadijk, A.A. Koelmans, Strong sorption of PCBs to nanoplastics, microplastics, carbon nanotubes, and fullerenes, Environmental Science and Technology. 48 (2014) 4869–4876. https://doi.org/10.1021/es405721v.
[17] L. Liu, R. Fokkink, A.A. Koelmans, Sorption of polycyclic aromatic hydrocarbons to polystyrene nanoplastic, Environmental Toxicology and Chemistry. 35 (2016) 1650–1655. https://doi.org/10.1002/etc.3311.
[18] Y. Ma, A. Huang, S. Cao, F. Sun, L. Wang, H. Guo, R. Ji, Effects of nanoplastics and microplastics on toxicity, bioaccumulation, and environmental fate of phenanthrene in fresh water, Environmental Pollution. 219 (2016) 166–173. https://doi.org/10.1016/j.envpol.2016.10.061.
[19] Q. Chen, D. Yin, Y. Jia, S. Schiwy, J. Legradi, S. Yang, H. Hollert, Enhanced uptake of BPA in the presence of nanoplastics can lead to neurotoxic effects in adult zebrafish, Science of The Total Environment. 609 (2017) 1312–1321. https://doi.org/10.1016/j.scitotenv.2017.07.144.
[20] C.-B. Jeong, H.-M. Kang, Y.H. Lee, M.-S. Kim, J.-S. Lee, J.S. Seo, M. Wang, J.-S. Lee, Nanoplastic Ingestion Enhances Toxicity of Persistent Organic Pollutants (POPs) in the Monogonont Rotifer Brachionus koreanus via Multixenobiotic Resistance (MXR) Disruption, Environmental Science and Technology. 52 (2018) 11411–11418. https://doi.org/10.1021/acs.est.8b03211.
[21] R. Jiang, W. Lin, J. Wu, Y. Xiong, F. Zhu, L.-J. Bao, J. You, G. Ouyang, E.Y. Zeng, Quantifying nanoplastic-bound chemicals accumulated in: Daphnia magna with a passive

dosing method, Environmental Science: Nano. 5 (2018) 776–781. https://doi.org/10.1039/c7en00932a.
[22] J. Liu, Y. Ma, D. Zhu, T. Xia, Y. Qi, Y. Yao, X. Guo, R. Ji, W. Chen, Polystyrene Nanoplastics-Enhanced Contaminant Transport: Role of Irreversible Adsorption in Glassy Polymeric Domain, Environmental Science and Technology. 52 (2018) 2677–2685. https://doi.org/10.1021/acs.est.7b05211.
[23] Q. Zhang, Q. Qu, T. Lu, M. Ke, Y. Zhu, M. Zhang, Z. Zhang, B. Du, X. Pan, L. Sun, H. Qian, The combined toxicity effect of nanoplastics and glyphosate on Microcystis aeruginosa growth, Environmental Pollution. 243 (2018) 1106–1112. https://doi.org/10.1016/j.envpol.2018.09.073.
[24] W. Lin, R. Jiang, Y. Xiong, J. Wu, J. Xu, J. Zheng, F. Zhu, G. Ouyang, Quantification of the combined toxic effect of polychlorinated biphenyls and nano-sized polystyrene on Daphnia magna, Journal of Hazardous Materials. 364 (2019) 531–536. https://doi.org/10.1016/j.jhazmat.2018.10.056.
[25] D. Kim, Y. Chae, Y.-J. An, Mixture Toxicity of Nickel and Microplastics with Different Functional Groups on *Daphnia magna*, Environmental Science & Technology. 51 (2017) 12852–12858. https://doi.org/10.1021/acs.est.7b03732.
[26] W.S. Lee, H.-J. Cho, E. Kim, Y.H. Huh, H.-J. Kim, B. Kim, T. Kang, J.-S. Lee, J. Jeong, Bioaccumulation of polystyrene nanoplastics and their effect on the toxicity of Au ions in zebrafish embryos, Nanoscale. 11 (2019) 3173–3185. https://doi.org/10.1039/C8NR09321K.
[27] L. Cai, L. Hu, H. Shi, J. Ye, Y. Zhang, H. Kim, Effects of inorganic ions and natural organic matter on the aggregation of nanoplastics, Chemosphere. 197 (2018) 142–151. https://doi.org/10.1016/j.chemosphere.2018.01.052.
[28] C.-S. Chen, C. Le, M.-H. Chiu, W.-C. Chin, The impact of nanoplastics on marine dissolved organic matter assembly, Science of the Total Environment. 634 (2018) 316–320. https://doi.org/10.1016/j.scitotenv.2018.03.269.
[29] L.-J. Feng, J.-J. Wang, S.-C. Liu, X.-D. Sun, X.-Z. Yuan, S.-G. Wang, Role of extracellular polymeric substances in the acute inhibition of activated sludge by polystyrene nanoparticles, Environmental Pollution. 238 (2018) 859–865. https://doi.org/10.1016/j.envpol.2018.03.101.
[30] O. Oriekhova, S. Stoll, Heteroaggregation of nanoplastic particles in the presence of inorganic colloids and natural organic matter, Environmental Science: Nano. 5 (2018) 792–799. https://doi.org/10.1039/c7en01119a.
[31] S. Summers, T. Henry, T. Gutierrez, Agglomeration of nano- and microplastic particles in seawater by autochthonous and de novo-produced sources of exopolymeric substances, Marine Pollution Bulletin. 130 (2018) 258–267. https://doi.org/10.1016/j.marpolbul.2018.03.039.
[32] O.S. Alimi, J. Farner Budarz, L.M. Hernandez, N. Tufenkji, Microplastics and Nanoplastics in Aquatic Environments: Aggregation, Deposition, and Enhanced Contaminant Transport, Environmental Science & Technology. 52 (2018) 1704–1724. https://doi.org/10.1021/acs.est.7b05559.
[33] J. Wu, R. Jiang, W. Lin, G. Ouyang, Effect of salinity and humic acid on the aggregation and toxicity of polystyrene nanoplastics with different functional groups and charges, Environmental Pollution. (2019) 836–843. https://doi.org/10.1016/j.envpol.2018.11.055.
[34] O. Pikuda, E.G. Xu, D. Berk, N. Tufenkji, Toxicity Assessments of Micro- and Nanoplastics Can Be Confounded by Preservatives in Commercial Formulations, Environmental Science & Technology Letters. 6 (2018) 21–25. https://doi.org/10.1021/acs.estlett.8b00614.

[35] G. Balakrishnan, M. Déniel, T. Nicolai, C. Chassenieux, F. Lagarde, Towards more realistic reference microplastics and nanoplastics: preparation of polyethylene micro/nanoparticles with a biosurfactant, Environmental Science: Nano. 6 (2019) 315–324. https://doi.org/10.1039/C8EN01005F.
[36] A.G. Rodríguez-Hernández, J.A. Muñoz-Tavares, C. Aguilar-Guzmán, R. Vazquez-Duhalt, Novel and simple method for polyethylene terephthalate (PET) nanoparticles production., Environ. Sci.: Nano. (2019). https://doi.org/10.1039/C9EN00365G.
[37] D.M. Mitrano, A. Beltzung, S. Frehland, M. Schmiedgruber, A. Cingolani, F. Schmidt, Synthesis of metal-doped nanoplastics and their utility to investigate fate and behaviour in complex environmental systems, Nature Nanotechnology. 14 (2019) 362–368. https://doi.org/10.1038/s41565-018-0360-3.
[38] L. Pessoni, C. Veclin, H.E. Hadri, C. Cugnet, M. Davranche, A.-C. Pierson-Wickmann, J. Gigault, B. Grassl, S. Reynaud, Soap- and metal-free polystyrene latex particles as a nanoplastic model, Environ. Sci.: Nano. 6 (2019) 2253–2258. https://doi.org/10.1039/C9EN00384C.
[39] D. Magrì, P. Sánchez-Moreno, G. Caputo, F. Gatto, M. Veronesi, G. Bardi, T. Catelani, D. Guarnieri, A. Athanassiou, P.P. Pompa, D. Fragouli, Laser Ablation as a Versatile Tool To Mimic Polyethylene Terephthalate Nanoplastic Pollutants: Characterization and Toxicology Assessment, ACS Nano. 12 (2018) 7690–7700. https://doi.org/10.1021/acsnano.8b01331.
[40] A.F. Astner, D.G. Hayes, H. O'Neill, B.R. Evans, S.V. Pingali, V.S. Urban, T.M. Young, Mechanical formation of micro- and nano-plastic materials for environmental studies in agricultural ecosystems, Science of The Total Environment. 685 (2019) 1097–1106. https://doi.org/10.1016/j.scitotenv.2019.06.241.
[41] M. Eriksen, M. Thiel, L. Lebreton, Nature of Plastic Marine Pollution in the Subtropical Gyres, in: H. Takada, H.K. Karapanagioti (Eds.), Hazardous Chemicals Associated with Plastics in the Marine Environment, Springer International Publishing, Cham, 2016: pp. 135–162. https://doi.org/10.1007/698_2016_123.
[42] J. Gigault, H. El, S. Reynaud, E. Deniau, B. Grassl, Asymmetrical flow field flow fractionation methods to characterize submicron particles: application to carbon-based aggregates and nanoplastics, Analytical and Bioanalytical Chemistry. 409 (2017) 6761–6769. https://doi.org/10.1007/s00216-017-0629-7.
[43] J. Sohma, Mechanochemistry of polymers, Progress in Polymer Science. 14 (1989) 451–596. https://doi.org/10.1016/0079-6700(89)90004-X.
[44] A. ter Halle, L. Ladirat, M. Martignac, A.F. Mingotaud, O. Boyron, E. Perez, To what extent are microplastics from the open ocean weathered?, Environmental Pollution. 227 (2017) 167–174. https://doi.org/10.1016/j.envpol.2017.04.051.
[45] L. Pessoni, C. Veclin, H. El Hadri, C. Cugnet, M. Davranche, A.-C. Pierson-Wickmann, J. Gigault, B. Grassl, S. Reynaud, Soap- and metal-free polystyrene latex particles as a nanoplastic model, Environmental Science: Nano. 6 (2019) 2253–2258. https://doi.org/10.1039/C9EN00384C.
[46] R.R. Retamal Marín, F. Babick, L. Hillemann, Zeta potential measurements for non-spherical colloidal particles – Practical issues of characterisation of interfacial properties of nanoparticles, Colloids and Surfaces A: Physicochemical and Engineering Aspects. 532 (2017) 516–521. https://doi.org/10.1016/j.colsurfa.2017.04.010.
[47] N. Wang, C. Hsu, L. Zhu, S. Tseng, J.-P. Hsu, Influence of metal oxide nanoparticles concentration on their zeta potential, Journal of Colloid and Interface Science. 407 (2013) 22–28. https://doi.org/10.1016/j.jcis.2013.05.058.
[48] N. Singh, E. Tiwari, N. Khandelwal, G.K. Darbha, Understanding the stability of nanoplastics in aqueous environments: Effect of ionic strength, temperature, dissolved organic

matter, clay, and heavy metals, Environ. Sci. Nano. 6 (2019) 2968–2976. https://doi.org/10.1039/c9en00557a.
[49] E. Kim, D. Lee, B. Yum, H. Chang, The effect of ionic strength and hardness of water on the non-ionic surfactant-enhanced remediation of perchloroethylene contamination, Journal of Hazardous Materials. 119 (2005) 195–203. https://doi.org/10.1016/j.jhazmat.2004.12.015.
[50] C. Della Torre, E. Bergami, A. Salvati, C. Faleri, P. Cirino, K.A. Dawson, I. Corsi, Accumulation and embryotoxicity of polystyrene nanoparticles at early stage of development of sea urchin embryos Paracentrotus lividus, Environmental Science and Technology. 48 (2014) 12302–12311. https://doi.org/10.1021/es502569w.
[51] S. Yu, M. Shen, S. Li, Y. Fu, D. Zhang, H. Liu, J. Liu, Aggregation kinetics of different surface-modified polystyrene nanoparticles in monovalent and divalent electrolytes, Environmental Pollution. 255 (2019) 113302. https://doi.org/10.1016/j.envpol.2019.113302.

CRediT author statement

Hind El Hadri: Conceptualization; Methodology ; Investigation; Formal analysis; Writing - Original Draft; Writing - Review & Editing; Visualization

Julien Gigault: Conceptualization; Formal analysis ; Writing - Original Draft; Funding acquisition

Benoit Maxit : Investigation

Bruno Grassl : Conceptualization ; Methodology ; Formal analysis; Writing - Original Draft; Writing - Review & Editing; Visualization; Supervision; Funding acquisition

Stéphanie Reynaud: Conceptualization ; Writing - Original Draft; Writing - Review & Editing; Project administration; Funding acquisition

Conceptualization	Ideas; formulation or evolution of overarching research goals and aims
Methodology	Development or design of methodology; creation of models
Software	Programming, software development; designing computer programs; implementation of the computer code and supporting algorithms; testing of existing code components
Validation	Verification, whether as a part of the activity or separate, of the overall replication/ reproducibility of results/experiments and other research outputs
Formal analysis	Application of statistical, mathematical, computational, or other formal techniques to analyze or synthesize study data
Investigation	Conducting a research and investigation process, specifically performing the experiments, or data/evidence collection
Resources	Provision of study materials, reagents, materials, patients, laboratory samples, animals, instrumentation, computing resources, or other analysis tools
Data Curation	Management activities to annotate (produce metadata), scrub data and maintain research data (including software code, where it is necessary for interpreting the data itself) for initial use and later reuse
Writing - Original Draft	Preparation, creation and/or presentation of the published work, specifically writing the initial draft (including substantive translation)
Writing - Review & Editing	Preparation, creation and/or presentation of the published work by those from the original research group, specifically critical review, commentary or revision – including pre-or postpublication stages
Visualization	Preparation, creation and/or presentation of the published work, specifically visualization/ data presentation
Supervision	Oversight and leadership responsibility for the research activity planning and execution, including mentorship external to the core team
Project	Management and coordination responsibility for the research activity

administration	planning and execution
Funding acquisition	Acquisition of the financial support for the project leading to this publication

Declaration of interests

☒ The authors declare that they have no known competing financial interests or personal relationships that could have appeared to influence the work reported in this paper.

☐The authors declare the following financial interests/personal relationships which may be considered as potential competing interests:

Graphical Abstract

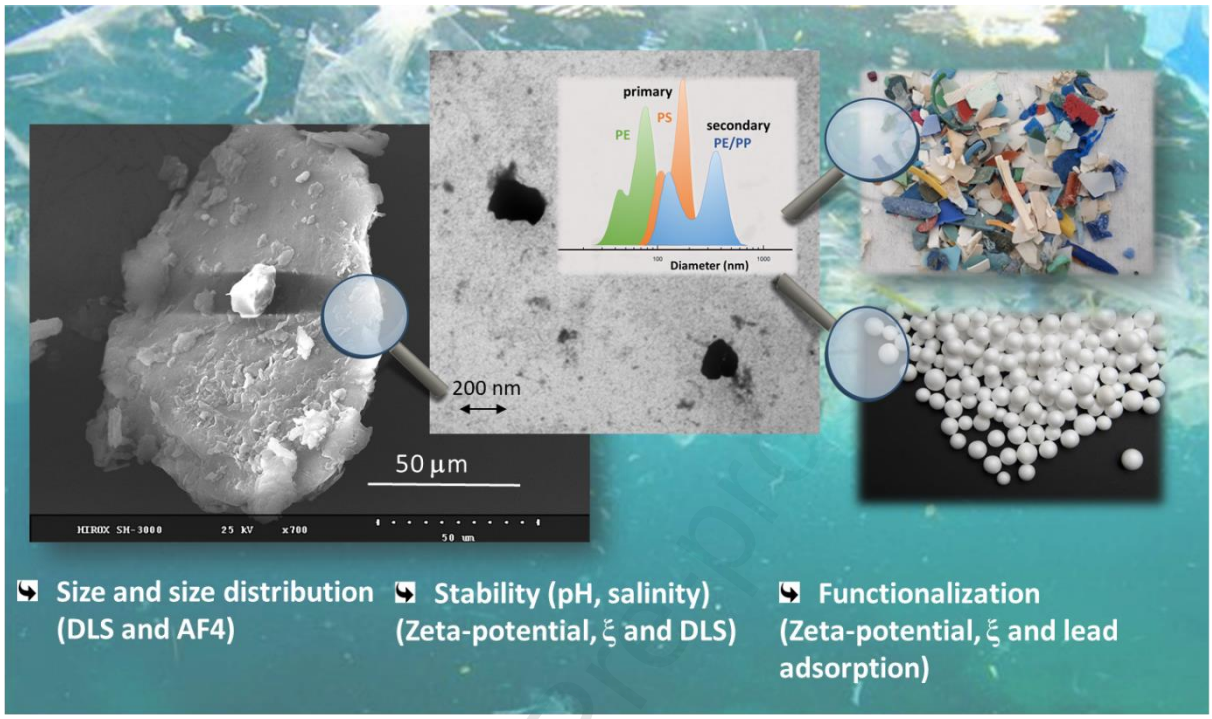

Highlights

- ~~A top-down method based on mechanical degradation providing new nanoplastics~~
- A top down method based on mechanical degradation providing randomly shaped nanoplastics
- ~~Analytic methodologies to characterize polydispersity, anisotropic shapes and negatively charged surfaces~~
- Production of polydisperse, anisotropic and negatively charged nanoplastics
- ~~Environmental assessment: nanoplastic stability and interaction with inorganic contaminant~~
- Nanoplastic stability assessment ~~and interaction with inorganic contaminant~~